International Journal of Engineering Applied Sciences and Technology, 2019
Vol. 4, Issue 5, ISSN No. 2455-2143, Pages 354-360

Ab INITIO INVESTIGATION OF $AgGaS_2$ and $AgGaSe_2$

Omehe N. N.
Department of Physics
Federal University, Otuoke
Bayelsa state, Nigeria

Omamoke O. E. Enaroseha
Department of Physics
Delta State University, Abraka
Delta State, Nigeria

Abstract- **The electronic structure optimization, electronic band structure, density of states and orbital decomposition of the density of states has been computed for $AgGaS_2$ and $AgGaSe_2$. The calculations were done employing the density functional theory (DFT), using the pseudopotential method with projector augmented wave (PAW). The LDA+U technique was used for the computations. The result of the optimization was found to be in good agreement with experimental findings. The results of the computations showed both materials to be semiconductors with direct band gap values of 1.82 eV and 1.25 eV for $AgGaSe_2$ and $AgGaS_2$ respectively. The calculated density of states and partial density of states revealed that the Ga-4s orbital has the highest energy while the Ga-3p orbital is the least in energy.**

Keywords – **Bandstructure, $AgGaS_2$, $AgGaSe_2$, DFT, Electronic band structure of $AgGaS_2$**

I. INTRODUCTION

$AgGaS_2$ (AGS) and $AgGaSe_2$ (AGSE) belong to the I-III-VI_2 system of compounds that semiconducting and have the chalcopyrite (tetragonal) structure. The materials under investigation are unique nonlinear crystals suitable for a wide range of three-wave mixing applications according to Catella and Burlage (1998). Hou et al, (2014), reported that their large nonlinear optical coefficient and high transmission in the infrared (IR) region makes them likely candidate for middle and deep IR applications, and efficient frequency doubling crystal for IR radiations, they are also potential candidate for blue chip excited LEDs and bio-labeling reported Huang et al, (2014). AGS and AGSE have attracted a lot of research interest from experimentalists and theorists.

One of the earliest researches into the properties of AGS and AGSE was done by Tell and Kasper, (1971). They investigated the optical and electrical properties of AGS and AGSE via luminescence and reflectivity measurements. They reported that both materials showed semiconducting properties with band gap values of 2.727 eV and 1.83 eV for AGS and AGSE respectively. Another early work investigating the electrical properties of AGS reported in the literature was that of Yu et al (1974), and it was reported that AGS is a p-type semiconductor.

Bai et al, (2004) did a first principle calculations of the linear and nonlinear properties of $AgGaX_2$ where X represents Sulphur S, Selenium Se and Tellurium Te. Their work was DFT based using pseudopotential method. The band structure calculated showed AGS and AGSE to be semiconductors with direct band gap of 2.230 eV and 1.421 eV respectively.

Hou et al, (2014) investigated the structure, optical and thermal properties of AGSE. They employed the ultra-soft pseudopotentials and used the generalized gradient approximation (GGA) for exchange and correlation. The result of their investigation predicted AGSE to be a direct band semiconductor with a value of 0.361 eV. This is way off the experimental value of 1.83 eV.

The work by Habanyama et al, (2015) involved the study of eight (8) chalcopyrite semiconductors inclusive of $AgGaS_2$ and $AgGaSe_2$. The Quantum suite of packages were used in the research, the values of the band gaps reported are 0.0 eV for $AgGaS_2$ and 0.1 eV for $AgGaSe_2$. A band gap of 0.9455 eV and 0.2234 eV were obtained for $AgGaS_2$ and $AgGaSe_2$ respectively by Chen et al (2007) in their DFT comparison study of $CuGaX_2$ and $AgGaX_2$, X being represented by S and Se.

Nano crystals of $AgGaS_2$ has also been reported in the literature (Huang et al, 2014; Paderick et al, 2018). Experimental studies of the optical properties of the materials in focus were reported in the literature (Catella and Burlage, 1998; Merschjann et al, 2012). Also reported were theoretical investigations of the optical properties of $AgGaS_2$ (Hai-Jun et al, 2010; Power et al, 2003; Brik, 2009). Yang et al (2018) reported the vibrational and thermal properties of $AgGaS_2$.

It should be noted that inspite of considerable literature, both experimental and theoretical on the materials under investigation, there is large variation of the reported band gap values. In this study, the structural and electronic band structure would be investigated.

II. COMPUTATION DETAILS

The ternary Chalcopyrites belongs to the space group D_{2d}^{12} (space group number 122). The Chalcopyrite structure is a superlattice of the Zinc-blende structure. The I-III-VI$_2$ chalcoprite has each group VI member [Sulphur (S), Selenium (S)] coordinated by two group I [Silver (Ag)] and two group III atoms [Gallium (Ga)]. Each group III atoms is tetrahedrally coordinated by four group VI atoms. Ga and Ag are at the 4a and 4b Wyckoff's atomic positions respectively. S or Se is at the 8d site as the case may be. The z value for AGS and AGSE is four (4), which gives a total of 16 atomic coordinates of three (3) types. Here, structure optimization, electronic band structure and charge transfer analysis were performed for AGS and AGSE. The pseudopotential method was used within the density functional theory (DFT) framework. The Abinit (ref) Quantum suite of packages was used in this study. In the structural optimizationof the materials under investigations, the starting lattice parameters were adopted from the experimental value 0ref). The x component of the 8d wyckoff'sposition was allowed to evolve while the others were fited. The self-consistency iterations continued until a force tolerance of 0.01 was reached. The optimization was done without the LDA+U component of the Abinit package. The results of the optimizations is shown in table 1. For the energy bands, total density of states (DOS), partial density of states (PDOS) and charge transfer, the LDA+U scheme was used with the projector augmented wave as implemented in the Abinit package. The following were states included in the computations, Ag has the 4s, 4p,4d and 5s orbitals, Ga has 3s,3p,3d, 4s and 4p while s and Se were represented by 4s,4p; and 3s, 3p states respectively. The plane waves were generated by a kenetic energy cut-off of 20 Ha, a Monkhorst-Pack shifted grid (ref) 4x4x4 yielding a mesh of 256 k-ponit. Which was used for the Brillioun zone intergration. The self-consistent computation was deemed to have achieved convergence when the energy tolerance of 10^{-8} was reached.

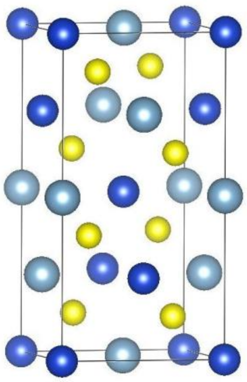

Figure 1: The structure used in the computations. Yellow balls represent S atoms, Blue balls for Ag atoms and Grey for Ga atoms.

Table 1: Optimization results

	a(Å)	**c(Å)**	***X***	***y***	***z***
AgGaS$_2$	5.7390	10.2702	0.0	0.0	0.0
			0.0	0.0	0.5
			u=0.2134	0.25	0.125
Experiment	5.75^a	10.29^a	u=0.282^b		
AgGaSe$_2$	5.9717	10.8745	0.0	0.0	0.0
			0.0	0.0	0.5
			u=0.2656	0.25	0.125
Experiment	5.98^a	10.88^a	u=0.272^b		

[a] Madelung (2004)

[b] Shay and Wernick (1975)

III. RESULTS AND DISCUSSIONS

The electronic band structure of AGS and AGSE are presented in figure 1 and 3 respectively. The Fermi energy is at the zero mark on the energy axis. The plot is energy against high symmetry points in the first Brillioun zone. The results of the computations showed AGS and AGSE to be semiconductors, this agrees with experimental results. The fundamental band gap is direct and occurs at the gamma point, which means that the conduction band minimum (CBM) and the valence band maximum (VBM) are both on the gamma point. The band gap value of AGS is 1.25 eV and AGSE is 1.82 eV. The calculated results for AGSE is in excellent agreement with experimental values of 1.814 eV (Madelung, 2004) and 1.83 eV (Tell and Kasper, 1971) and also in excellent agreement with the theoretical result of Bai et al, (2004) who reported a value of 2.23 eV. The calculated band gap value for AGS is about 1.464 eV shy of the experimental value of 2.714 reported by (handbook) and 1.477 eV difference from what Tell and Kasper reported, but in good agreement with the theoretical result of Bai et al (2004) who obtained a band gap value of 1.421 eV. Table 2 shows the comparative transition energies along lines of high symmetry for AGS and AGSE

Table 2: Comparative transition energies along lines of high symmetry for AGS and AGSE

	E_g(eV)	E_g^M (eV)	E_g^P (eV)	E_g^X (eV)
AGS	1.25	1.93	2.16	1.93
AGSE	1.82	2.73	2.67	2.61
Experiment				
AGS	2.714			2.7
AGSE	1.814			

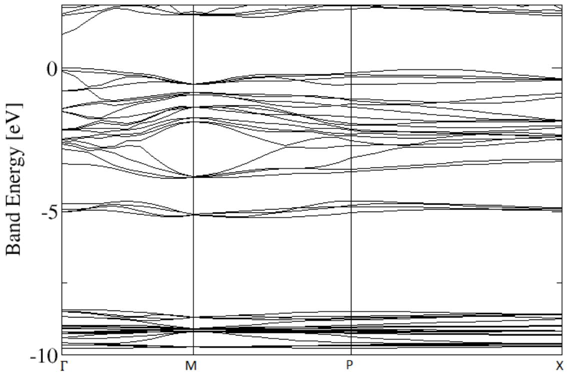

Figure 2: Electronic band structure of $AgGaS_2$. The Fermi energy is at the zero mark.

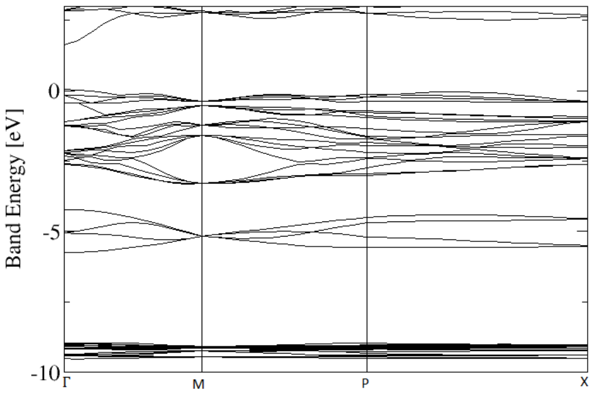

Figure 3: Electronic band structure of $AgGaSe_2$. The Fermi energy is at the zero mark.

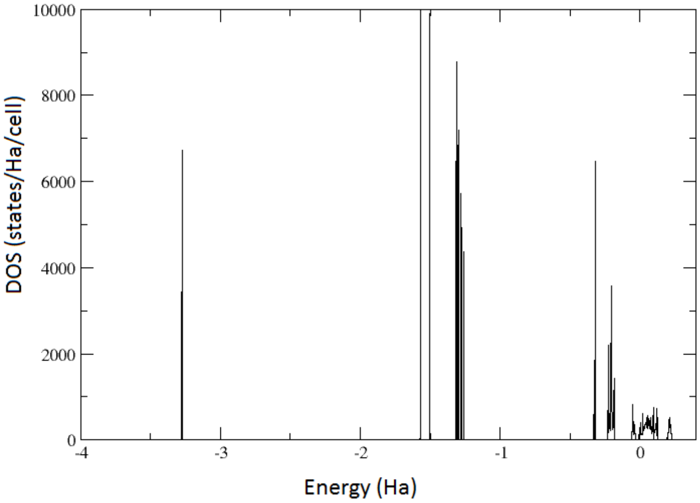

Figure 4: Total density of states for $AgGaS_2$. he Fermi energy is at 0.13 Ha.

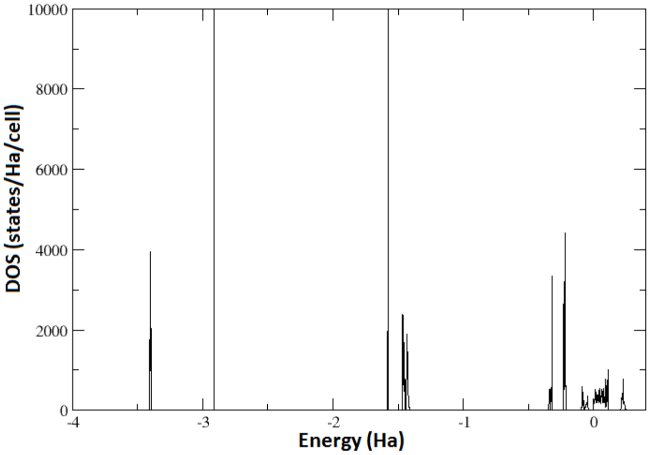

Figure 5: Total density of states for $AgGaSe_2$. The Fermi energy is at 0.13 Ha.

Figures 4 and 5 is the display of the respective density of states, like the band structure, the energy is clear well reproduced. This shows agreement and accuracy of the computation. The orbital decomposition of the density of states for $AgGaS_2$ and $AgGaSe_2$ into the various orbital contributions are shown in figures 6 to 11. For $AgGaS_2$, the orbital contribution from Ag to the total density of states are the 4s, 4p, 4d and 5s orbitals. These various contributions are presented in figure 6. The partial density of state of the 4d orbital is clearly seen in figure 6a and it occupies the energy range of about – 0.3 Ha to 0.15 Ha. They are the dominant orbital within this energy range. The p orbital contribution come by way of the 4p states and it is shown in figure 6b. Its energy dispersion is very narrow. It is one of the core states included the computations as semi-core. The contribution of the s orbital, the 4s and the 5s is shown in figure 6c. The dispersion of the 4s orbital is narrow as shown in the figure. The peak close to the – 3.0 Ha represents the 4s state. The 5s state is found around the Fermi energy and it energy dispersion is from about – 0.30 Ha to the Fermi energy level. The partial density of states from Ga are shown in figure 7. Figure 7a represents contribution from the 3d states. These states are represented within the energy range of – 1.30 to – 1.50 Ha. The p orbital contribution is from the 3p and 4p. The states around – 3.30 Ha describes the 3p while the states about – 0.30 to 0.0 represents 4p orbitals, with a very small contribution to the conduction states. This conduction band is seen as a peak after the energy gap. The 4s orbital has significant contributions to the density of states as revealed in figure 7c. The 4s orbital has significant states about the valence states immediately before the Fermi energy and also across the energy band gap. The S-3p states are the dominant states in the valence bands immediately before the Fermi energy level. They also have significant states in the conduction band, this is shown in figure 8a. The S-3s orbital contribution is within the energy range o – 0.30 Ha to – 0.1 Ha, with a sharp peak at – 0.30 Ha. It has contributions to the valence band as well as the conduction band, albeit contributions to the conduction band are quite small as described in figure 8b.

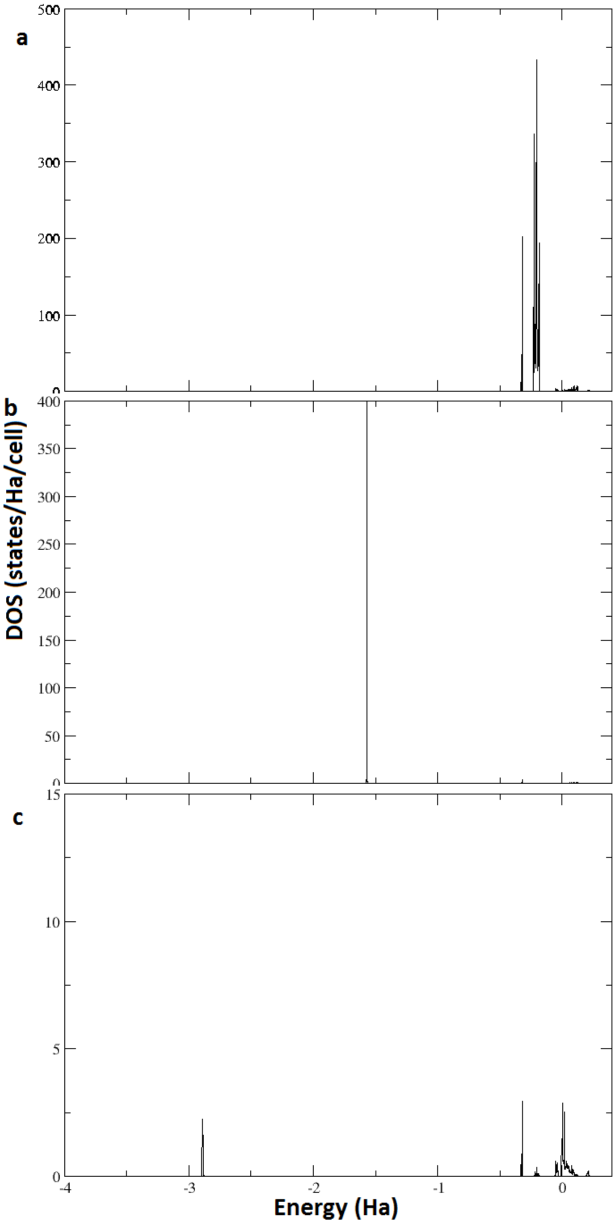

Figure 6: The partial density of states for the Ag atoms in $AgGaS_2$. (a) the Ag-4d partial-DOS (b) Ag-4p partial DOS (c) Ag-4s and Ag-5s partial DOS.

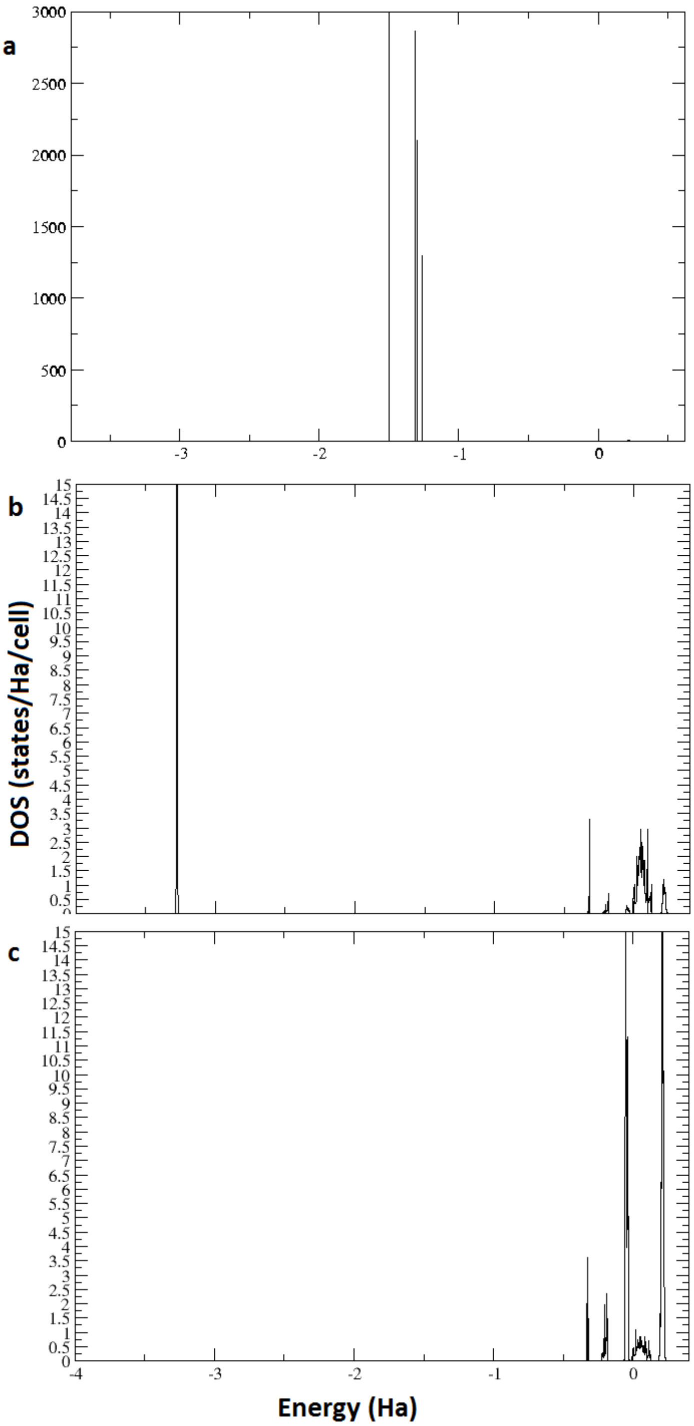

Figure 7: The partial density of states for the Ga atoms in $AgGaS_2$. (a) Ga-3d partial-DOS (b) Ga-3p and Ga-4p partial DOS (c) Ga-4s partial DOS.

Figure 9 shows the partial density of states of the orbital contribution of Ag to the total density of state of $AgGaS_2$. Here, the expected contribution is from the 4s, 4p, 4d and 5s orbitals. Figure 9a represents the 4d states with energy between -0.2 Ha to-

0.3 Ha, figure 9b reflects the 4p contributions. Its is around -1.6 Ha. Its energy spread is narrow, hence, a sharp peak. The 4s and 5s partial density of state are shown in figure 9c. The 4s representation is further down the scale than the 4p orbital contribution. This is seen at – 2.9 Ha mark.

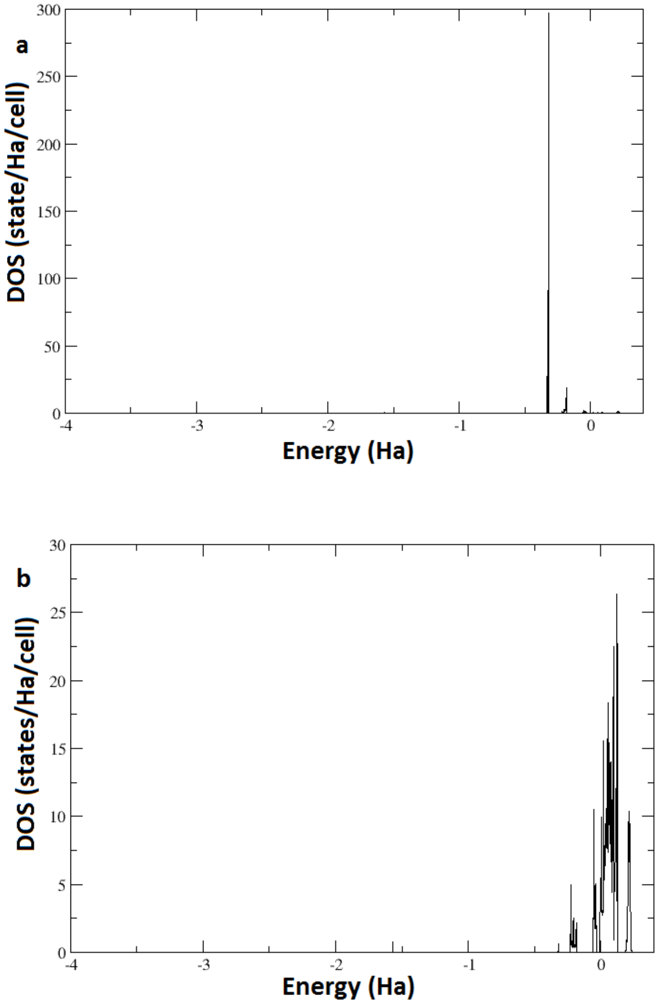

Figure 8: The partial density of states for the S atoms in $AgGaS_2$. (a) The S-3s partial-DOS (b) S-3p partial DOS

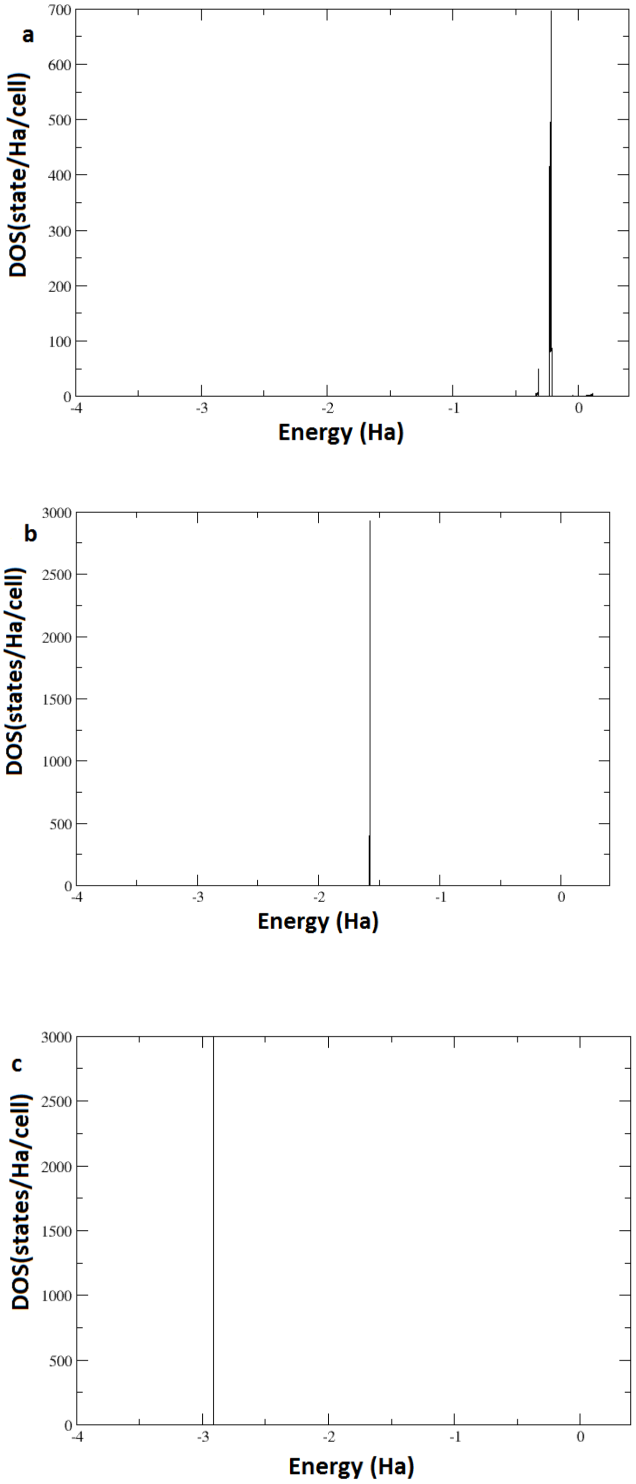

Figure 9: The partial density of states for the Ag atoms in $AgGaSe_2$. (a) Ag-4d partial-DOS (b) Ag-4p partial DOS (c) Ag-4s and Ag-5s partial DOS.

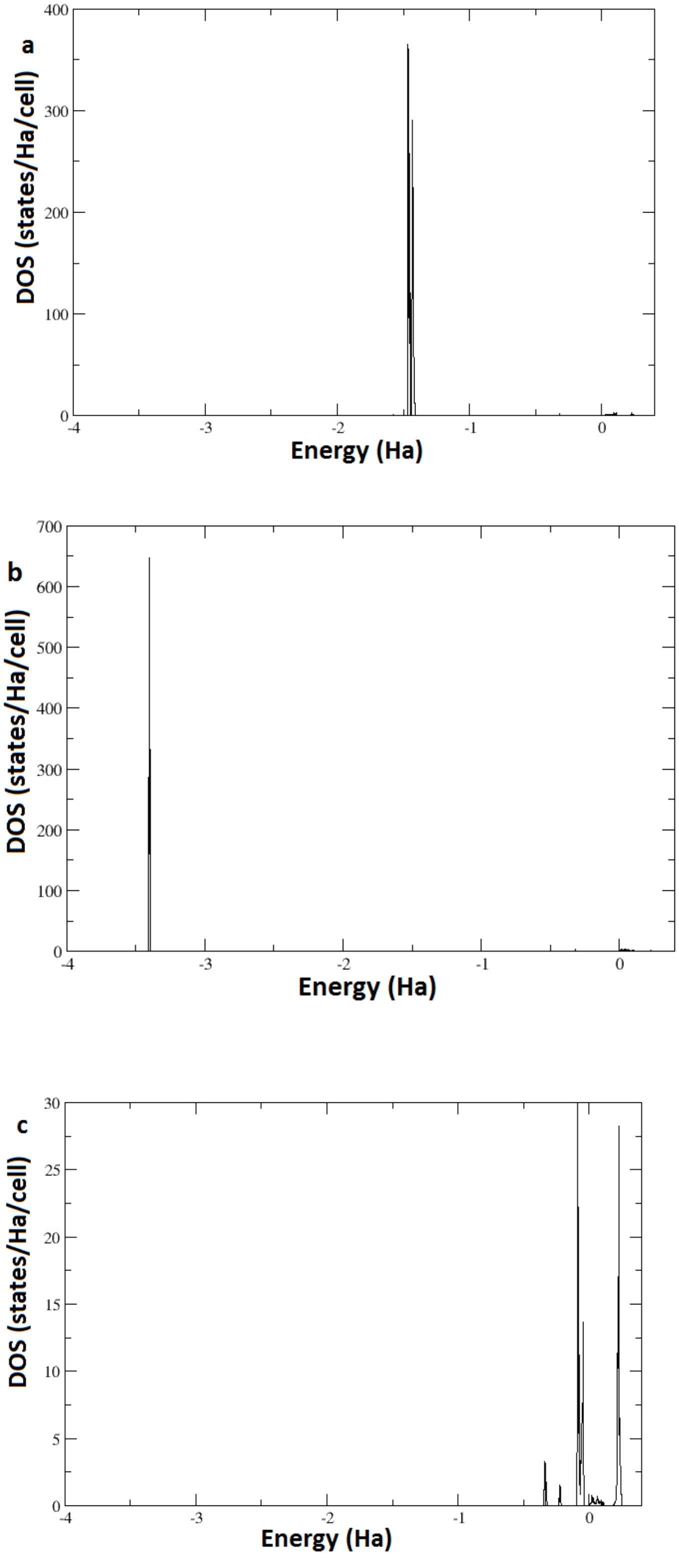

Figure 10: The partial density of states for the Ga atoms in AgGaSe$_2$. (a) Ga-3d partial-DOS (b) Ga-3p and Ga-4p partial DOS (c) Ga-4s partial DOS.

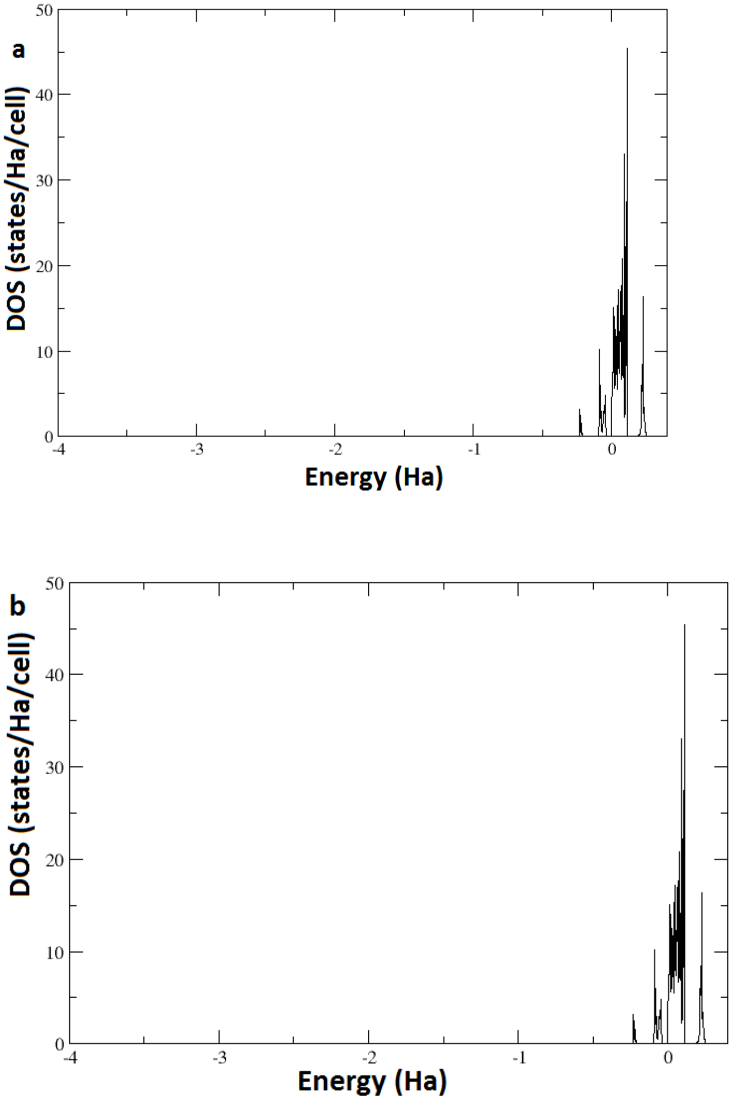

Figure 11: The partial density of states for the S atoms in AgGaSe$_2$. (a) The S-3s partial-DOS (b) S-3p partial DOS

Figure 10 displays the contributions from the Ga states, 3p, 3d, 4s and 4p to the total density of states. Figure 10a shows the density of states from the 3d orbitals, while figures 10b and 10c show the partial density of states for the 3p and 4p; and 4s states respectively. The 3d energy dispersion range is from – 0.5 Ha to – 0.4 Ha. The 3p orbital is at an energy level further down the energy scale close – 0.3.5 Ha mark. The 4p states can be clearly seen as states close to the Fermi level, though this contribution is quite small. The Ga-3p states are seen to occupy the least enery level. This is clear when compared to the total density of states in figure 5. Contributions from the Ga-4s and Se-4p are the dominant states around the Fermi level, that is, states immediately before the Fermi energy. There are also significant in the conduction band. This is shown in figure 10c and 11a. The Se-3s state is concentrated at – 0.14 energy level with some contributions close to the Fermi level. A very small portion is also in the conduction band.

IV. CONCLUSION

We have used density functional theory (DFT) in conjunction with the pseudopotential method, the projector augmented wave (PAW) and the LDA+U technique to compute the electronic properties of $AgGaS_2$ and $AgGaSe_2$. Our calculates revealed that both materials are semiconductors with direct band gap. Our results are in good agreement with experimental investigations.

V. REFERENCES

1. Habanyama A., Silungme D., Phiri E. and Manyala R. O. (2015), Computational study of the Electronic and Structural Properties of Semiconductors with Chalcopyrite Structure, Africa Rev. of Phys 10, pp 291-301.
2. Tell B. and Kasper H. M. (1971), Optical and Electrical properties of $AgGaS_2$ Phys. Rev. **B**, 4 issue 12, pp 4455-4459.
3. Merschjann C., Mews M., Mete T., Karkatzinou A., Rusu M., Korzun B. V., Schorr S., Schubert – Bischoff P., Seeger S., Schedel-Niedrig Th. and M-Ch Lux-Steiner (2012), $AgGaSe_2$ Thin Films Grown by Chemical Close-spaced Vapour Transport for Photovoltaic Applications: Structural, Compositional and Optical Properties, Journ. of Phys., condensed matter, vol. 24, No. 17
4. Power Ch., Gilliland S., Segura A. and Gonzales J. (2003), Variation of the optical absorption edge in $AgGaS_2$ Single Crystals at High Pressure, Physica Status Solidi (b), vol. 235, issue 2.
5. Huang F., Zhou J., Xu J. and Wang Y. (2014), Formation of $AgGaS_2$ Nano – pyramids from Ag_2S Nanospheres through Intermediate Ag_2S – $AgGaS_2$ Heterostructures and $AgGaS_2$ Sensitized Mn^{+2} Emission, Nanoscale, 6, 2340 – 2344.
6. Catella G. C. and Burlage D. (1998), Crystal Growth and Optical Properties of $AgGaS_2$ and $AgGaSe_2$, MRS Bulletin, vol. 23, issue 7, pp 28-36.
7. Gonze X., Beuken J.-M., Caracas R., Detraux F., Fuchs M., Rignanese G.-M., Sindic L., Verstraete M., Zerah G., Jollet F., Torrent M., Roy A., Mikami M., Ghosez Ph., Raty J.-Y., and Allan D.C., First-principles computation of material properties : the Abinit software project, Computational Materials Science 25, 478-492 (2002).
8. Gonze X., Rignanese G.-M., Verstraete M., Beuken J.-M., Pouillon Y., Caracas R., Jollet F., Torrent M., Zerah G., Mikami M., Ghosez Ph., Veithen M., Raty J.-Y., Olevano V., Bruneval F., Reining L., Godby R., Onida G., Hamann D. R., and Allan D. C., A brief Introduction to the Abinit software package. Z. Kristallogr. 220, 558-562 (2005).
9. Hai-Jun H., Shi-Fu Z., Bei-Jun Z., Yu Y. and Lin-Hua X. (2010), First-Principle Calculations of the Elastic, Electronic and Optical Properties of $AgGaS_2$, Physica Scripta, vol. 82, number 5, pp 055601.
10. Hou H.. J., Kong F. J., Yang J. W., Xie L. H. and Yang S. X. (2014), First – Principle Study of the Structural, Optical and Thermal Properties of $AgGaSe_2$, Phys. Scr. 89, pp 065703-065710.
11. Shay J. L. and Wernick J. H. (1975), Ternary Chalcopyrite Semiconductors: Growth, Electronic Properties and applications, Pergamon press, Oxford.
12. Yang J., Fan Q., Yu Y. and Zhang W. (2018), Pressure Effect of the Vibrational and Thermodynamics Properties of Chalcopyrite_type Compound $AgGaS_2$, materials 11 (12) 2370 – 2382.
13. Bai L., Lin Z., Wang Z. and Chen C. (2004), Mechanism of Linear and Nonlinear effects of Chalcopyrite $AgGaX_2$ (X=S, Se, Te) crystals, Journal of Chem. Phys. Vol. 120, number 18, pp 8772-8778.
14. Brik M. G. (2009), First-Principle Study of the Electronic and Optical Properties of $CuXS_2$ (X = Al, Ga, In) and $AgGaS_2$, Journ. of Phys.: condensed matter, vol. 21 No. 48
15. Madelung O. (2004), Semiconductors: Data Hand book, Springer, 3rd edition.
16. Yu P. W., Manthuruthil J. and Park Y. S. (1974), Some Properties of $AgGaS_2$, Journ. of Apl. Phys. 45, pp 3694-3696.
17. Chen S., Gong X. G. and Wei S-H. (2007), Band-Structure Anomalies of the Chalcopyrite Semiconductors $CuGaX_2$ Versus $AgGaX_2$ (X = S and Se) and their Alloys, Phys. Rev. **B** 75, pp 205209 – 205218.
18. Endo S., Noda Y. and Furukawa Y. (1993), Transpiraation Experiment of $AgGaS_2$, Jap. Journ. of Appl. Phys., vol. 32, pt 1, number 5A.
19. Paderick S., Kessler M., Hurlburt T. J. and Hughes S. M. (2018), Synthesis and Characterization of $AgGaS_2$ Nanoparticles: A Study of Growth and Fluorescence, Chem. Commun., 62 – 65.